

Contents lists available at [SciVerse ScienceDirect](http://www.sciencedirect.com)

Composites: Part B

journal homepage: www.elsevier.com/locate/compositesb

Plasma functionalization of bucky paper and its composite with phenylethynyl-terminated polyimide

Qian Jiang^{a,b}, Yishuang Li^{a,b}, Jianfei Xie^{a,b}, Jie Sun^{a,b}, David Hui^c, Yiping Qiu^{a,b,*}

^a Key Laboratory of Textile Science and Technology, Ministry of Education, China

^b College of Textiles, Donghua University, Shanghai 201620, China

^c Department of Mechanical Engineering, University of New Orleans, New Orleans, LA 70148, USA

ARTICLE INFO

Article history:

Received 22 April 2012

Accepted 14 June 2012

Available online xxx

Keywords:

B. Mechanical properties

B. Thermal properties

Carbon nanotubes

A. Nano-structures

B. Surface properties

ABSTRACT

The present study presents the fabrication and performance of plasma functionalized bucky paper reinforced phenylethynyl-terminated polyimide (PETI). Multi-wall carbon nanotubes in the form of bucky papers are functionalized using He/O₂ plasma, and the effect is revealed by XPS and wettability test, showing improved hydrophilicity on the bucky paper surface. For the nanocomposites made with PETI, the functionalized sample exhibits a 30% increase in tensile strength and 125% increase in tensile modulus compared with those of the untreated samples, indicating improved adhesion between the bucky paper and PETI. The thermal properties of the composites are unchanged before and after the plasma treatment. No substantial mass loss is observed below 500 °C in oxygen, indicating high temperature resistance of the composite.

© 2012 Elsevier Ltd. All rights reserved.

1. Introduction

Much attention has been paid to macroscopic assemblies of carbon nanotubes (CNTs), in order to take full advantage of theoretically ultra-strong individual CNTs. CNTs in macroscopic scale have potentials in functional applications, such as supercapacitor [1,2], sensor and electrode [3,4], and structural applications [5] when combined with traditional reinforcement fabrics. Bucky paper, in the form of multiwall carbon nanotube (MWCNT) cake, can be made in a large size suitable for macroscopic applications [6]. However, the individual MWCNTs in a bucky paper are held together by Van der Waals forces, the weakest among all intermolecular forces [7]. MWCNTs in a bucky paper reinforced composite are impregnated in a matrix such that the mechanical properties of MWCNTs can be utilized more efficiently [8]. For a MWCNT composite, creating good interface between the MWCNTs and the polymer matrix is critical for achieving effective load transfer [9]. Better interface can be obtained through selectively functionalizing nanotube using acid chemically binding MWCNTs to polymers [10–12]. However, this will bring in impurities and cause defects in MWCNT when strong acid is applied, such as H₂SO₄, HNO₃, HCl [13]. In comparison, plasma treatments have been used as an environmentally friendly means to treat various types of material surfaces without altering their bulk properties [14,15]. In plasma treatments, ex-

cited radicals, electrons and ions break the chemical bonds and create active groups for binding with polymers [16]. Different plasma atmospheres can produce a wide range of functional groups with high efficiency, meeting various demands in industrial applications [17]. Recently, studies have been carried out to plasma functionalize CNTs or MWCNTs in different atmospheres and with different parameters. Felten et al. [18] modified CNTs with radio-frequency plasma in O₂, NH₃ and CF₄ atmospheres. It was found that, when the optimal values of the plasma parameters were applied, functional groups (hydroxide, carbonyl, carboxyl, amine, fluorine, etc.) were created on the CNT surfaces while no damage to the CNTs was observed. Chen et al. [19] functionalized MWCNTs by microwave-excited surface wave oxygen plasma and found that the Ar/O₂ plasma treatment greatly enhanced the content of oxygen, modified structural properties and improved the dispersion of MWCNTs in aqueous solutions. More surface defects were induced while the integrity of the nanotube patterns was not damaged. Vohrer et al. modified CNTs and bucky papers using Ar/N₂/O₂ plasma and found that the oxygen containing plasma atmosphere improved the hydrophilicity of CNT surfaces [20].

Phenylethynyl-terminated polyimide (PETI) was firstly introduced by Harris et al. [21]. This thermosetting polyimide has been used for high-speed civil transportation (HSCTs) applications due to its desirable properties [22]. PETI-5 was developed by NASA Langley Research Center and was regarded as one of the best high performance polymers for composite matrix [23]. Several researchers have worked on changing oligomers to improve the polymer properties. Connell and coworkers developed two phenylethynyl

* Corresponding author at: College of Textiles, Donghua University, Shanghai 201620, China.

E-mail address: ypqiu@dhu.edu.cn (Y. Qiu).

terminated oligomers designated PETI-298 and PETI-330 as the leading candidates for composite applications requiring high temperature performance (i.e. $\geq 88^\circ\text{C}$ for 1000 h) [24]. Ogasawara et al. synthesized Triple-A PI by replacing the symmetric 3,3',4,4'-biphenyltetracarboxylic dianhydride (s-BPDA) by asymmetric 2,3,3',4'-biphenyltetracarboxylic dianhydride (a-BPDA) and fabricated composites reinforced with MWCNTs. Their experimental results showed increased elastic modulus and yield strength, and the glass transition temperature went up with incorporation of the carbon nanotubes, suggesting that the MWCNTs were acting as macroscopic crosslinks and further immobilized the polyimide chains at elevated temperatures [25]. These studies focus on random carbon nanotube reinforced polyimide composite by mixing CNTs with polyimide similar to the process of making a regular short fiber composite, which could not achieve a high volume fraction of CNTs. However, a bucky paper, as an assembly of MWCNT, could have much higher nanotube loading levels, up to 50% [26], and great potential for composite property improvement [27]. Fu et al. incorporated the bucky paper onto the surface of polyimide/carbon fiber composites. The bucky paper/polyimide layer worked as an excellent physical barrier, obstructing the flow of heat and oxygen into the bulk of the composite [28].

Relatively few researchers have studied plasma modification of carbon nanotubes for reinforcing polymer composites. Pötschke et al. studied Ar/O₂ plasma functionalized bucky paper and polycarbonate composites [29]. Tseng et al. and Chen et al. used plasma modification for random CNTs to reinforce epoxy composites [30,31]. They concluded that the modification increased both the mechanical and electrical properties. However, little has been reported in literature about plasma modification of CNTs or bucky paper for PI matrix composites.

The aim of this paper is to investigate the effect of He/O₂ plasma functionalization of a MWCNT bucky paper on the mechanical properties of its corresponding polyimide composite. The surface chemical composition of the bucky paper before and after the plasma treatment was determined by X-ray photoelectron spectrometry (XPS). The surface morphology and surface wettability of the bucky paper were examined using scanning electron microscopy (SEM) and static water contact angle measurement. The mechanical properties of the bucky paper/PETI composite were also tested.

2. Experimental

2.1. Bucky paper production

MWCNTs was supplied by Tsinghua University (average diameter of 20 nm, purity >90%, according to the supplier). The aspect ratios of the individual MWCNT are in the range of 25–30. Following the bucky paper preparation process described in literature [32], 150 mg MWCNT was dispersed utilizing ultrasonication under 53 KHz for 1.5 h in 150 ml methanol solution with 0.1% Triltron X-100 (purchased from Sinopharm Chemical Reagent Co. Ltd.) as the surfactant. The solution was vacuum-filtrated under 0–0.1 MPa with a PTFE filter membrane (0.22 μm mean pore size) and washed with methanol to remove the residual Triltron X-100. The bucky paper (diameter 64 mm, thickness 70 μm) was peeled off after drying under 120 $^\circ\text{C}$ for 1 h. The control and the plasma treated samples were made under the same condition using the same batch of MWCNTs to ensure a consistent volume fraction.

2.2. Plasma functionalization

An atmospheric pressure plasma jet (APPJ) Atomflo™-R (Surfex Technologies, CA) was used to treat the bucky paper. A capacitively coupled electrode design was employed in the device to produce

stable discharge with 13.56 MHz radio frequency power at atmospheric pressure. It was reported that pure oxygen plasma created the highest oxygen content but disrupted the CNT structure [20]. Therefore, this experiment adopted mixed gas of helium/oxygen (100:1 ratio) at a flow rate of 20/0.2 l/min with a power of 40 W. The samples were placed on a conveying belt moving at a speed of 6 mm/s, and the distance between the sample and the nozzle was 2–3 mm, which was the most effective distance according to our previous studies [33]. Plasma treatment to a porous structure could be effective both in interior and exterior surfaces [34] depending on the penetration depth of the plasma in bucky paper which was approximately 5 nm [20]. The samples were treated on both sides for 1 lap (8s), keeping the inner graphite structure undamaged [29].

2.3. Phenylethynyl-terminated polyimide synthesis

The oligomers used in this study were 4,4'-oxydipthalic anhydride (ODPA), 4,4'-methylenedianiline (MDA) obtained from Shanghai Research Institute of Synthetic Resins, and 4-(Phenylethynyl)phthalic anhydride (PEPA) supplied by Changzhou Sunlight Pharmaceutical Company. OPDA was dehydrated in vacuum oven at 160 $^\circ\text{C}$ for 8 h to avoid degradation by water in synthesis. Methanol, as the solvent, was dehydrated by molecular sieve before use. The imide oligomer was prepared at a calculated molecular weight of 1500 g/mole with a molar ratio of ODPA:MDA:PEPA = 1.78:2.78:2.00. The reaction is shown in Fig. 1. ODPA, MDA and PEPA were extracted in methanol separately and then mixed by stirring for 4 h, forming brown, viscous poly(amide) acid.

2.4. Composite preparation

The untreated and treated bucky papers were mixed with poly(amide) acid at 80 $^\circ\text{C}$ using vacuum filtration method. Therefore the infiltration of poly(amide) acid into the bucky papers was improved compared with the traditional cast method. The obtained prepregs were put into molds, pressed under 1 kPa and heated in a vacuum oven following a stepwise program (Fig. 2) to remove residual solvent and compact the composite structure.

2.5. Scanning electron microscopy analysis

The morphological structures of the bucky papers and composites were inspected using a scanning electron microscope (Hitachi S-4800). Different resolutions were chosen to observe the morphology change after the plasma treatment.

2.6. Surface wettability analysis

Wettability measurement was performed using Video-Based Optical Contact Angle Meter (Dataphysics, OCA15EC). Distilled water was used as the liquid for the static water contact angle measurement.

2.7. X-ray photoelectron spectroscopy analysis

The surface chemical compositions of plasma-treated and untreated bucky papers were analyzed using an XPS system (Thermo ESCALAB 250) equipped with a Mg Ka X-ray source with pass energy of 1253.6 eV. The analysis was carried out under 10^{-9} – 10^{-10} Torr with power of 300 W. Photo emitted electrons were collected at a take-off angle of 45 $^\circ$ and the deconvolution analysis of C1s peaks was carried out using XPS Peak software.

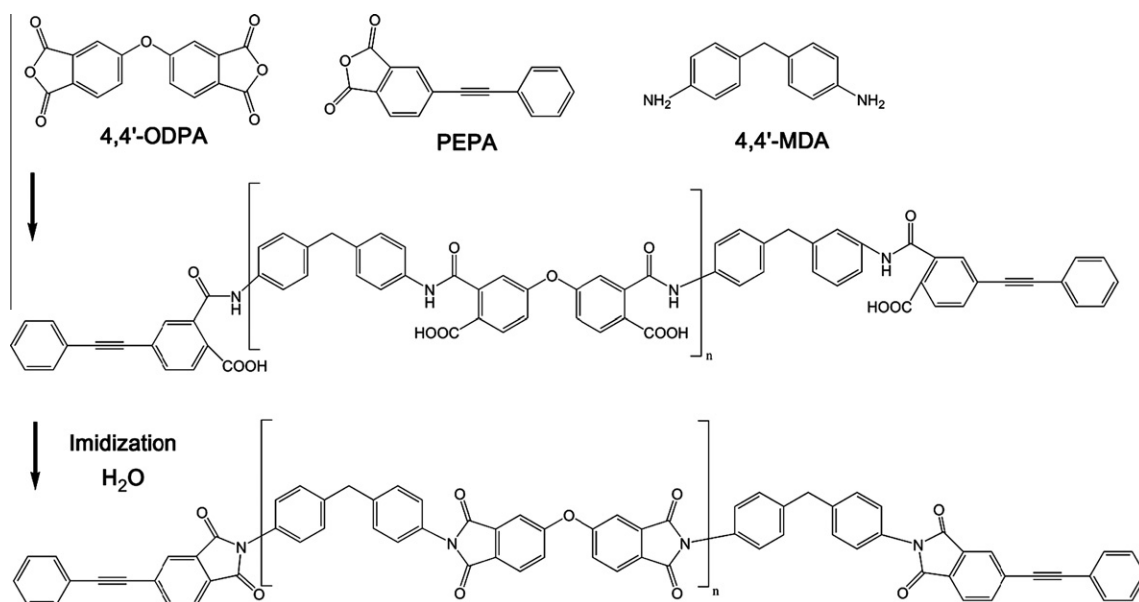


Fig. 1. Synthetic scheme of the imide oligomers from the reaction ODPA, MDA and PEPA.

2.8. Mechanical property test

Stress–strain behavior of the composites was tested using a tensile testing machine (Shimadzu EZ-S). The crosshead speed and the gauge length were 0.5 mm/min and 6 mm, respectively. The samples were cut into strips with a dimension of 0.3 mm wide and 10 mm long.

2.9. Thermogravimetric analysis

Thermo-stability of the bucky paper/PETI composites was assessed by Thermogravimetric analysis (NETZSCH, TG209 F1). The tests were run from 25 to 900 °C at 15 °C/min in air. The specimens were tested in air in order to simulate the application conditions in real world applications.

3. Results and discussion

3.1. Surface morphology of bucky paper

SEM images of the untreated bucky paper (a) and the plasma treated bucky paper and (b) are shown in Fig. 3. The uniform dispersion was observed in these images, because systematic studies were carried out on solvent and dispersant concentration in our previous work and optimal parameters were used in this study. It is interesting to find that there was no significant difference between the plasma treated and the control samples except the areas shown in circles where the carbon nanotubes were “cut” by plasma and more ends showed up. But this “cutting” effect may not significantly influence the bucky paper property since all “cutting” could only happen on the surface. Unlike the acid treatment which could damage the CNTs [35], the integrity of MWCNT bundles in bulk of

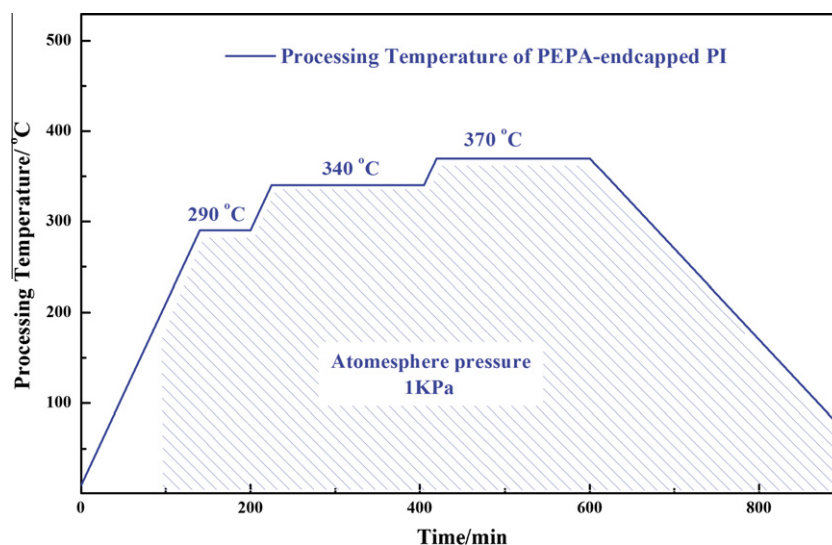


Fig. 2. Hot-pressing stage of bucky paper/phenylethynyl-terminated polyimide composite.

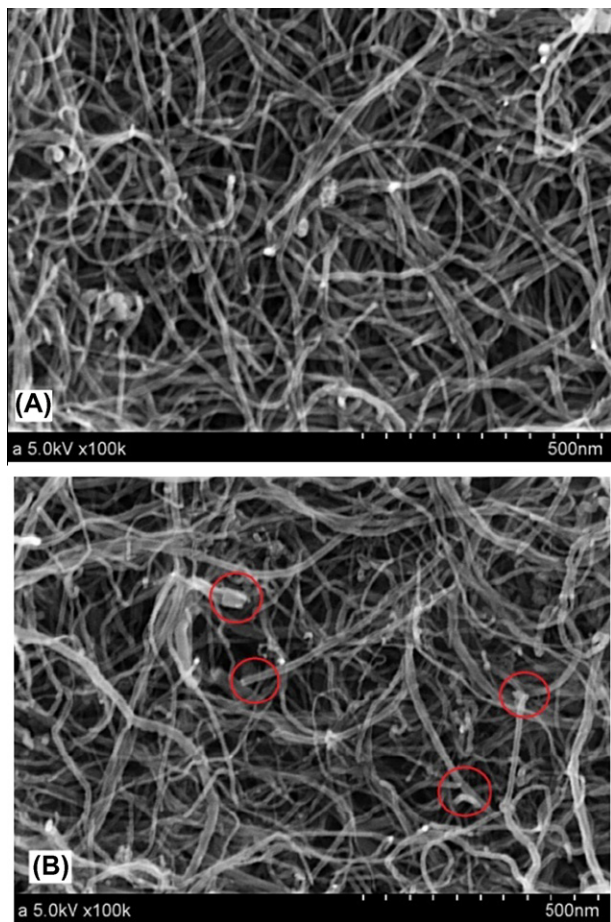


Fig. 3. SEM images of untreated (A) and plasma treated and (B) buckypaper.

the bucky paper was maintained after the plasma treatment. Besides, the surface ends could increase the mechanical interlocking between the bucky paper and the polymer after composite was made, which was called nanomechanical interlocking [36], thus improving the mechanical properties of the composite.

3.2. Surface chemical composition and wettability change

XPS analysis was conducted to identify the surface chemical composition changes of the bucky paper after plasma functionalization. The C1s spectra were deconvoluted into five characteristic Gaussian peaks (Fig. 4), including sp^2 -hybridized graphite-like carbon atoms (284.1 ± 0.2 eV), sp^3 -hybridized graphite-like carbon atoms (285.1 ± 0.2 eV), C–O (286.2 ± 0.2 eV), C=O (287.2 ± 0.2 eV) and O=C–O (288.9 ± 0.2 eV) [19]. The C–O, C=O and O=C–O groups observed on the bucky paper surface were likely resulted from plasma induced oxidation as well as surface contamination or impurities. As shown in Table 1, C=C, C=O and O=C–O ratios slightly decreased after plasma treatment, while C–C and C–O increased somewhat. This indicates that the graphene structure on the surface of the MWCNT was partially disrupted after the plasma treatment since C=C should only exist in the graphene structure.

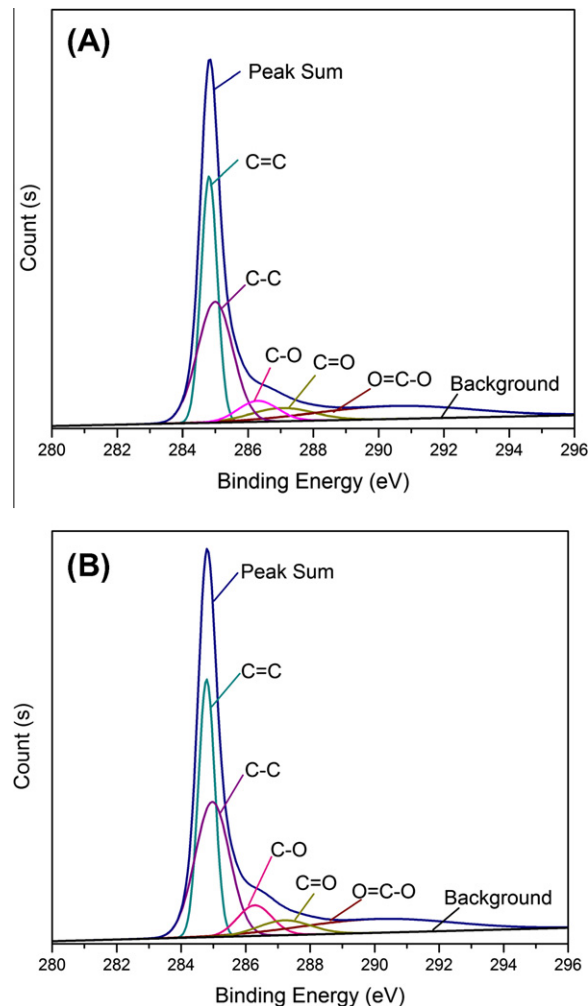


Fig. 4. XPS C1s spectrum of untreated (A) and oxygen plasma-treated and (B) bucky paper.

Felten et al. theoretically calculated the bonding energies of the functional groups identified by XPS as shown in the following sequence: CNT–OH (116 kcal/mol) > CNT–COOH (80 kcal/mol) > CNT=O (70 kcal/mol) > CNT=C=O (–36 kcal/mol) [37]. Therefore in this study, CNT–OH should less likely to be degraded by the plasma than CNT–COOH and CNT=O, which explained why the number of C=O and O=C–O decreased whereas C–O increased. In oxygen plasma atmosphere, free radicals were also created on the surface of the bucky paper, promoting the reaction with polyimide. The 20% increase of C–O fraction should lead to an improved hydrophilicity of the MWCNT since CNT–OH is a more hydrophilic side group than C=O and O=C–O.

In order to determine how much the plasma treatment transformed hydrophobic surfaces to hydrophilic surfaces for the bucky paper, the water contact angle tests were performed and the results are shown in Fig. 5. Water contact angles decreased from 125.4° for the control to 34.9° for the plasma treated sample. It gives us a clear evidence of wettability change, which is due to

Table 1
Relative percentage of five components of carbon atoms and calculated ratio of carbon and oxygen atoms.

| | C=C (%) | C–C (%) | C–O (%) | C=O (%) | O=C–O (%) | [C]/[O] |
|----------------|---------|---------|---------|---------|-----------|---------|
| Untreated | 33.77 | 35.72 | 6.92 | 6.89 | 16.70 | 8.16 |
| Plasma-treated | 32.91 | 36.41 | 8.33 | 6.08 | 16.27 | 5.40 |

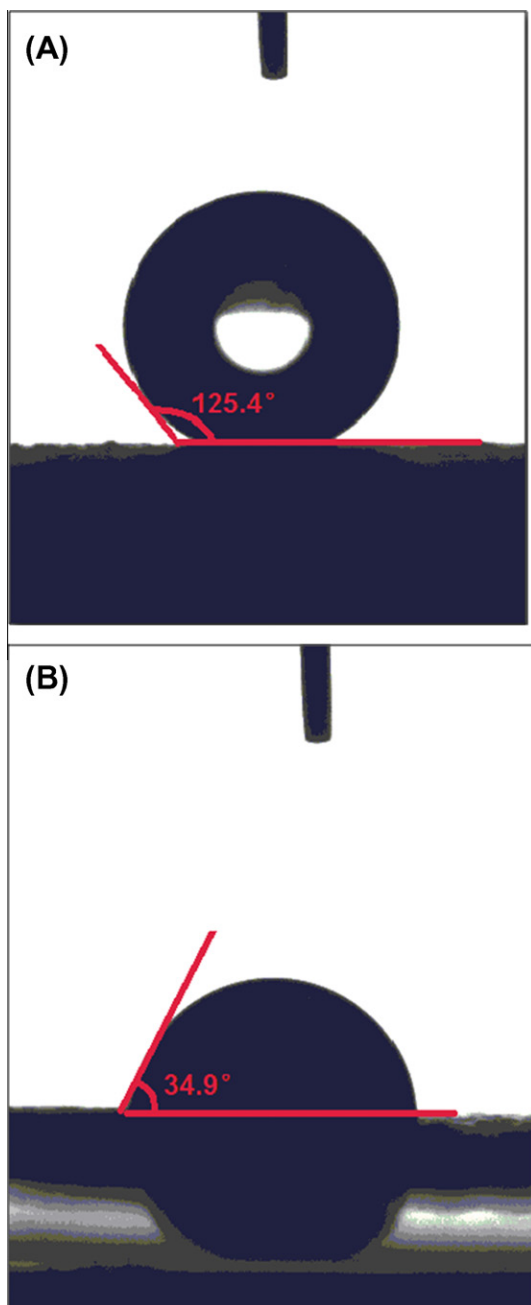


Fig. 5. Contact angle measurement of bucky before (A) and after (B) oxygen plasma treatment.

more C–O groups induced by the plasma treatment. The increased C–O group should make the resin infusion easier and fiber/resin interface stronger, resulting in improved mechanical and physical properties of the composites.

3.3. Composite mechanical properties

Typical stress–strain curves of the control and the plasma-modified bucky paper/PETI composites are shown in Fig. 6. The untreated bucky paper/PETI exhibited a failure stress of 208 MPa and an elastic modulus of 17.6 GPa. After the plasma functionalization, the failure stress and the elastic modulus increased to 271 MPa and 39.6 GPa, rising 30% and 125% respectively. The strength and failure strain of the pure PETI were around 100 MPa and 8%, respectively as reported by Bryant et al. [38] and Ogasawara et al. [25].

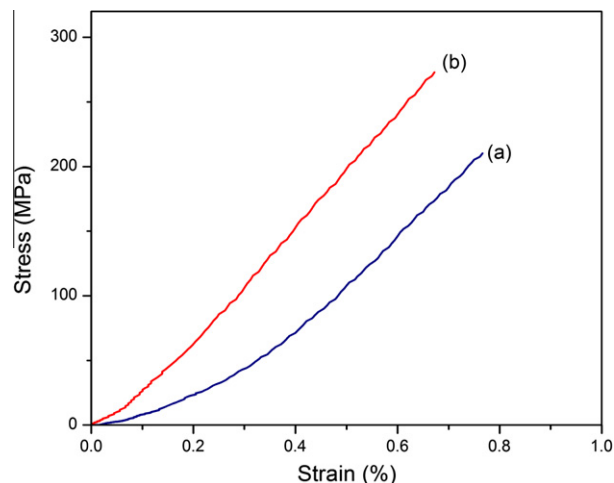


Fig. 6. Stress–strain curve of bucky paper/PETI composite (a) untreated and (b) plasma treated.

It indicates that carbon nanotube more effectively reinforced the matrix and increased the mechanical properties. Qian et al. estimated the elastic modulus of MWCNT/PS composite using an in-plane randomly oriented discontinuous fiber lamina model [39]. Ogasawara et al. chose three-dimensional analysis based on Eshelby–Mori–Tanaka theory [40], taking into account the effect of three-dimensional random orientation and entangled distribution of nanotubes [25]. According to the latter model, the estimated elastic modulus should be around 38 GPa [25], close to the plasma functionalized sample in this study. That indicates that the modulus of composite without plasma functionalization was far below the estimated value, resulting from the poor stress transfer between the matrix and the MWCNTs. Comparing the two samples before and after the plasma functionalization, a significant increase in elastic modulus was obtained. This improvement may be attributed to the increased interfacial adhesion between the MWCNTs and PETI due to the increased number of C–O groups on the MWCNTs [30].

The SEM images of fractured composite surfaces are shown in Figs. 7 and 8. The improved infiltration and thus adhesion between bucky paper and phenylethynyl-terminated polyimide was observed. Fig. 7 gives the cross section of the bucky paper/phenylethynyl-terminated polyimide. Resin rich areas were found on both sides of composite. While in the tube rich region, the MWCNT

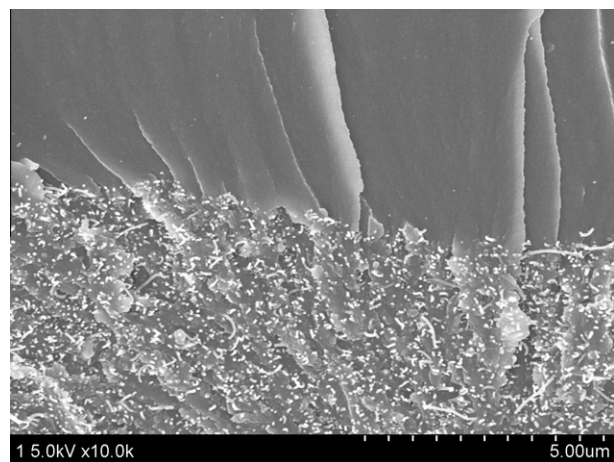


Fig. 7. Cross section of bucky paper/phenylethynyl-terminated polyimide. Resin rich areas are found on both sides of composite.

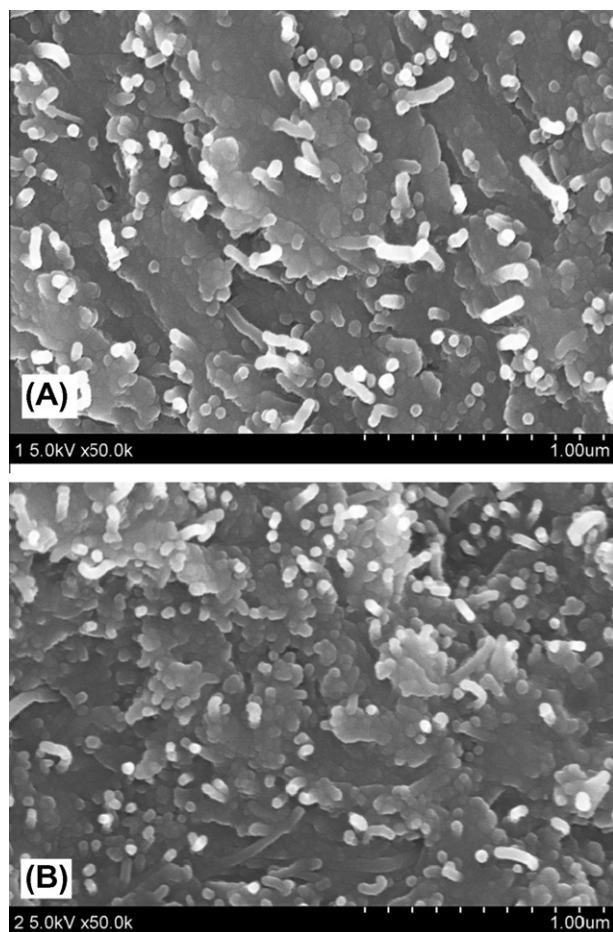


Fig. 8. Fracture surface of bucky paper/PETI composite before (A) and after (B) plasma functionalization, indicating the adhesion improvement.

volume fraction was about 25%, the overall volume fraction of the composite could be around 10% due to the existence of the resin rich regions. Fig. 8 provides the magnified view of the MWCNT rich regions of the fractured composite surfaces. As shown in Fig. 8a, for the control sample, long and free nanotube ends are manifested, indicating MWCNTs were pulled out easily during the tensile test because of the poor adhesion. In contrast, as shown in Fig. 8b, after plasma functionalization, the broken nanotube ends in the fractured composite surface became shorter, implying an improved bonding between the MWCNTs and the resin.

3.4. Thermal properties

As shown in Fig. 9, the TGA curve for the composite made of plasma functionalized bucky paper was not significantly different from that of the control sample. There was almost no weight loss before 500 °C even in air, indicating high temperature resistance of the composites. The subtle decrease of mass percentage (seen in the dashed frame) from 200 °C to 600 °C reflects the increase of oxygen-containing groups. According to the literature [41], oxygen-containing groups are stable under 200 °C, irrespective of the functionalizing methods applied. In decomposition above 200 °C, CO₂ and H₂O were produced at low temperatures and H₂ and CO were generated at high temperatures [41]. Nevertheless, this slight reduction of mass may not significantly influence the thermal property of the composite. In other words, the heat resistance of the composite was maintained after plasma functionalization of the bucky paper.

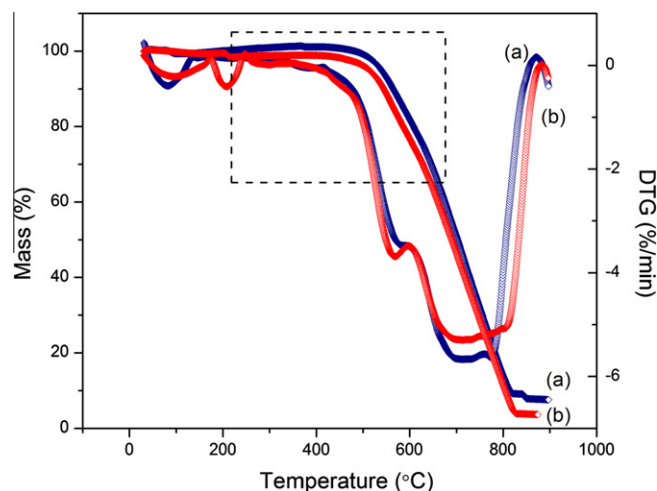


Fig. 9. Thermogravimetric analysis curve of bucky paper/PETI composite: (a) unmodified and (b) plasma modified.

4. Conclusion

Plasma functionalization was applied successfully on bucky paper to modify the surface composition. The bucky paper/PETI composites were well infiltrated when using vacuum filtration method. After plasma treatment, the hydrophilic groups on the bucky paper were increased, resulting in a more hydrophilic surface. The nano-mechanical interlocking mechanism takes effect during tensile loading. The combination of the above two effects were beneficial to the improvement of mechanical properties between MWCNTs and PETI. Thermal gravimetric analysis showed high temperature resistance of bucky paper/PETI composites regardless plasma functionalization of the bucky paper.

Acknowledgements

This work was supported by the National High Technology Research and Development Program of China (No. 2007AA03Z101), the State Key Program of National Natural Science of China (No. 51035003), Natural Science Foundation for the Youth (Nos. 50803010 and 60904056), National Science Foundation for Post-doctoral Scientists of China (No. 20100470664), Shanghai Post-doctoral Research Funded Project (No. 09R21410100), the Program of Introducing Talents of Discipline to Universities (No. B07024), Shanghai University Young Teacher Training Program and the Fundamental Research Funds for the Central Universities.

References

- [1] An KH, Jeon KK, Heo JK, Lim SC, Bae DJ, Lee YH. *J Electrochem Soc* 2002;149:A1058–62.
- [2] An KH, Kim WS, Park YS, Choi YC, Lee SM, Chung DC, et al. *Adv Mater* 2001;13:497–500.
- [3] Li J, Cassell A, Delzeit L, Han J, Meyyappan M. *J Phys Chem B* 2002;106:9299–305.
- [4] Inpil K et al. *Smart Mater Struct* 2006;15:737.
- [5] Veedu VP, Cao A, Li X, Ma K, Soldano C, Kar S, et al. *Nat Mater* 2006;5:457–62.
- [6] Rinzler AG, Liu J, Dai H, Nikolaev P, Huffman CB, Rodríguez-Macías FJ, et al. *Appl Phys A: Mater* 1998;67:29–37.
- [7] Liu J, Rinzler AG, Dai H, Hafner JH, Bradley RK, Boul PJ, et al. *Science* 1998;280:1253–6.
- [8] Wang Z, Liang Z, Wang B, Zhang C, Kramer L. *Compos Part A: Appl Sci Manuf* 2004;35:1225–32.
- [9] Breuer O, Sundararaj U. *Polym Composite* 2004;25:630–45.
- [10] Eitan A, Jiang K, Dukes D, Andrews R, Schadler LS. *Chem Mater* 2003;15:3198–201.
- [11] Velasco-Santos C, Martínez-Hernández AL, Fisher FT, Ruoff R, Castaño VM. *Chem Mater* 2003;15:4470–5.

- [12] Zhu J, Kim J, Peng H, Margrave JL, Khabashesku VN, Barrera EV. *Nano Lett* 2003;3:1107–13.
- [13] Osorio AG, Silveira ICL, Bueno VL, Bergmann CP. *Appl Surf Sci* 2008;255:2485–9.
- [14] Guruvanket S, Rao GM, Komath M, Raichur AM. *Appl Surf Sci* 2004;236:278–84.
- [15] Oh KW, Kim SH, Kim EA. *J Appl Polym Sci* 2001;81:684–94.
- [16] Ionescu R, Espinosa EH, Sotter E, Llobet E, Vilanova X, Correig X, et al. *Sens Actuators B: Chem* 2006;113:36–46.
- [17] Ryan ME, Badyal JPS. *Macromolecules* 1995;28:1377–82.
- [18] Felten A, Bittencourt C, Pireaux JJ, Van Lier G, Charlier JC. *J Appl Phys* 2005;98:074308.
- [19] Chen C, Liang B, Ogino A, Wang X, Nagatsu M. *J Phys Chem C* 2009;113:7659–65.
- [20] Vohrer U, Zschoerper NP, Koehne Y, Langowski S, Oehr C. *Plasma Process Polym* 2007;4:S871–7.
- [21] Harris FW, Pamidimukkala A, Gupta R, Das S, Wu T, Mock G. *J Macromol Sci Part A Chem* 1984;21:1117–35.
- [22] N.R.C.Co.H.S. Research. *US supersonic commercial aircraft: assessing NASA's high speed research program*. National Academies Press; 1997.
- [23] Hergenrother PM, Smith Jr JG. *Polymer* 1994;35:4857–64.
- [24] Connell JW, Smith JG, Hergenrother PM, Criss JM. *High Perform Polym* 2003;15:375–94.
- [25] Ogasawara T, Ishida Y, Ishikawa T, Yokota R. *Compos Part A: Appl Sci Manuf* 2004;35:67–74.
- [26] Gonnet P, Liang Z, Choi ES, Kadambala RS, Zhang C, Brooks JS, et al. *Curr Appl Phys* 2006;6:119–22.
- [27] Coleman JN, Khan U, Blau WJ, Gun'ko YK. *Carbon* 2006;44:1624–52.
- [28] Fu X, Zhang C, Liu T, Liang R, Wang B. *Nanotechnology* 2010;21:235701.
- [29] Pötschke P, Zschoerper NP, Moller BP, Vohrer U. *Macromol Rapid Commun* 2009;30:1828–33.
- [30] Tseng C-H, Wang C-C, Chen C-Y. *Chem Mater* 2006;19:308–15.
- [31] Chen IH, Wang C-C, Chen C-Y. *Plasma Process Polym* 2010;7:59–63.
- [32] Rinzler AG, Liu J, Dai H, Nikolaev P, Huffman CB, Rodríguez-Macías FJ, et al. *Appl Phys A: Mater Sci Process* 1998;67:29–37.
- [33] Wang CX, Ren Y, Qiu YP. *Surf Coat Technol* 2007;202:77–83.
- [34] Masuoka T, Hirasa O, Suda Y, Ohnishi M. *Int J Radiat Appl Inst Part C: Radiat Phys Chem* 1989;33:421–7.
- [35] Marshall MW, Popa-Nita S, Shapter JG. *Carbon* 2006;44:1137–41.
- [36] Xu X, Thwe MM, Shearwood C, Liao K. *Appl Phys Lett* 2002;81:2833–5.
- [37] Felten A, Bittencourt C, Pireaux JJ, Van Lier G, Charlier JC. *J Appl Phys* 2005;98.
- [38] Bryant RG, Jensen BJ, Hergenrother PM. *J Appl Polym Sci* 1996;59:1249–54.
- [39] Qian D, Dickey EC, Andrews R, Rantell T. *Appl Phys Lett* 2000;76:2868–70.
- [40] Mori T, Tanaka K. *Acta Metall* 1973;21:571–4.
- [41] Polovina M, Babic B, Kaluderovic B, Dekanski A. *Carbon* 1997;35:1047–52.